

Fate of trace organic compounds in the hyporheic zone: influence of retardation, the benthic bio-layer and organic carbon

Jonas Schaper, Malte Posselt, Camille Bouchez, Anna Jaeger, Gunnar Nuetzmann, Anke Putschew, Gabriel Singer, Jörg Lewandowski

▶ **To cite this version:**

Jonas Schaper, Malte Posselt, Camille Bouchez, Anna Jaeger, Gunnar Nuetzmann, et al.. Fate of trace organic compounds in the hyporheic zone: influence of retardation, the benthic bio-layer and organic carbon. Environmental Science and Technology, 2019, 53 (8), pp.4224-4234. 10.1021/acs.est.8b06231 . insu-02082924

HAL Id: insu-02082924
https://insu.hal.science/insu-02082924

Submitted on 28 Mar 2019

HAL is a multi-disciplinary open access archive for the deposit and dissemination of scientific research documents, whether they are published or not. The documents may come from teaching and research institutions in France or abroad, or from public or private research centers.

L'archive ouverte pluridisciplinaire **HAL**, est destinée au dépôt et à la diffusion de documents scientifiques de niveau recherche, publiés ou non, émanant des établissements d'enseignement et de recherche français ou étrangers, des laboratoires publics ou privés.

Environmental Science & Technology

Subscriber access provided by SCD Université de Rennes1 | SCD de l'Université de Rennes 1

Environmental Processes

Fate of trace organic compounds in the hyporheic zone: influence of retardation, the benthic bio-layer and organic carbon

Jonas Schaper, Malte Posselt, Camille Bouchez, Anna Jaeger, Gunnar Nützmann, Anke Putschew, Gabriel Singer, and Jörg Lewandowski

Environ. Sci. Technol., **Just Accepted Manuscript** • Publication Date (Web): 24 Mar 2019

Downloaded from http://pubs.acs.org on March 28, 2019

Just Accepted

"Just Accepted" manuscripts have been peer-reviewed and accepted for publication. They are posted online prior to technical editing, formatting for publication and author proofing. The American Chemical Society provides "Just Accepted" as a service to the research community to expedite the dissemination of scientific material as soon as possible after acceptance. "Just Accepted" manuscripts appear in full in PDF format accompanied by an HTML abstract. "Just Accepted" manuscripts have been fully peer reviewed, but should not be considered the official version of record. They are citable by the Digital Object Identifier (DOI®). "Just Accepted" is an optional service offered to authors. Therefore, the "Just Accepted" Web site may not include all articles that will be published in the journal. After a manuscript is technically edited and formatted, it will be removed from the "Just Accepted" Web site and published as an ASAP article. Note that technical editing may introduce minor changes to the manuscript text and/or graphics which could affect content, and all legal disclaimers and ethical guidelines that apply to the journal pertain. ACS cannot be held responsible for errors or consequences arising from the use of information contained in these "Just Accepted" manuscripts.

ACS Publications

is published by the American Chemical Society. 1155 Sixteenth Street N.W., Washington, DC 20036

Published by American Chemical Society. Copyright © American Chemical Society. However, no copyright claim is made to original U.S. Government works, or works produced by employees of any Commonwealth realm Crown government in the course of their duties.

Fate of trace organic compounds in the hyporheic zone: influence of retardation, the benthic bio-layer and organic carbon

JONAS L. SCHAPER[1,2]*, MALTE POSSELT,[3] CAMILLE BOUCHEZ,[4] ANNA JAEGER,[1,5] GUNNAR NUETZMANN,[1,5] ANKE PUTSCHEW,[2] GABRIEL SINGER,[1] AND JOERG LEWANDOWSKI[1,5]

[1] Leibniz-Institute of Freshwater Ecology and Inland Fisheries, Department Ecohydrology, Müggelseedamm 310, 12587 Berlin, Germany

[2] Technische Universität Berlin, Chair of Water Quality Engineering, Strasse des 17. Juni 135, 10623 Berlin, Germany

[3] Department of Environmental Science and Analytical Chemistry (ACES), Stockholm University, Stockholm, Sweden

[4] Univ Rennes, CNRS, Géosciences Rennes, UMR 6118, 35000 Rennes, France

[5] Humboldt University Berlin, Geography Department, Rudower Chaussee 16, 12489 Berlin, Germany

*corresponding author; schaper@igb-berlin.de, Leibniz-Institute of Freshwater Ecology and Inland Fisheries, Department Ecohydrology, Müggelseedamm 310, 12587 Berlin, Germany

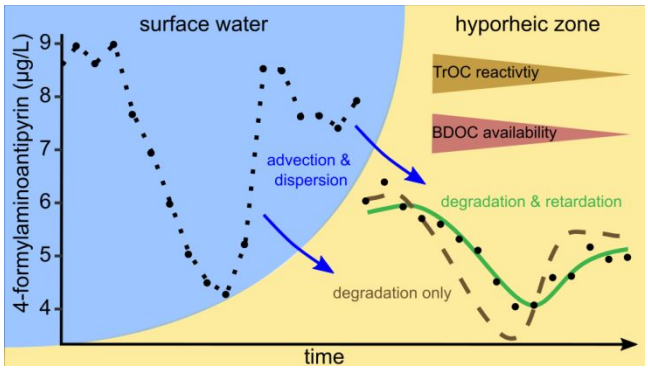
Abstract

The fate of 28 trace organic compounds (TrOCs) was investigated in the hyporheic zone (HZ) of an urban lowland river in Berlin, Germany. Water samples were collected hourly over 17 h in the river and in three depths in the HZ using minipoint samplers. The four relatively variable time series were subsequently used to calculate first-order removal rates and retardation coefficients via a one-dimensional reactive transport model. Reversible sorption processes led to substantial retardation of many TrOCs along the investigated hyporheic flow path. Some TrOCs such as dihydroxy-carbamazepine, O-desmethylvenlafaxine and venlafaxine were found to be stable in the HZ. Others were readily removed with half-lives in the first 10 cm of the HZ ranging from 0.1±0.01 h for iopromide to 3.3±0.3 h for tramadol. Removal rate constants of the majority of reactive TrOCs were highest in the first 10 cm of the HZ, where removal of biodegradable dissolved organic matter was also highest. Because conditions were oxic along the top 30 cm of the investigated flow path we attribute this finding to the high microbial activity typically associated with the shallow HZ. Frequent and short vertical hyporheic exchange flows could therefore be more important for reach-scale TrOC removal than long, lateral hyporheic flow paths.

Keywords

Pharmaceuticals, metformin, guanylurea, urban water cycle, reactive transport modeling

TOC Art



Introduction

Many trace organic compounds such as pharmaceuticals are only partially retained in wastewater treatment plants (WWTPs)[1,2] and thus are ubiquitous in urban surface waters.[3,4] In rivers, TrOCs are of eco-toxicological concern[5–7] and the high persistence of some TrOCs in aquatic environments poses issues for drinking water production.[8] The hyporheic zone (HZ), the portion of the streambed in which surface waters and groundwater mix,[9] is generally regarded as an effective bioreactor, characterized by steep redox gradients, diverse microbial communities and relatively high microbial turnover rates.[10,11] Both laboratory[12,13] and field studies[14,15] demonstrated that the HZ is able to efficiently remove many TrOCs, even along relatively short flow paths (< 20 cm). Therefore, the HZ may not only act as a filter protecting groundwater form surface water contamination[16] but also contributes to whole-stream, i.e. reach-scale attenuation of TrOCs.[17]

The adequate assessment of the in-situ efficiency of the HZ in removing TrOCs requires a sound understanding of both the in-situ reactivity and the exposure time of TrOCs to favorable attenuation conditions. Hyporheic residence times are predominately controlled by transport characteristics such as porewater velocity and dispersion. However, residence times of TrOCs along hyporheic flow paths may also be influenced by sorption and desorption processes, i.e. retardation.[18–20] Retardation can extend residence times of TrOCs in the HZ and, if not considered in reactive transport modeling, may lead to an overestimation of the in-situ reactivity of TrOCs in the HZ. Although retardation of some TrOCs in saturated sediments has been demonstrated in laboratory studies[20,21] little is known about its driving factors and its overall importance for transport of TrOCs in hyporheic sediments.

Reactivity of TrOCs in the HZ increases with temperature[12] and, for many TrOCs, is higher under oxic conditions.[12,14] However, since microbially mediated degradation and transformation mechanisms are considered to be a main driver of TrOC removal in saturated sediments, it is likely that TrOC reactivity in the HZ is also linked to microbial activity and growth and therefore to turnover of biodegradable dissolved organic matter (BDOC).[22] It has been shown that microbial activity in the HZ is typically highest in the

shallow HZ (within the so called benthic bio-layer), where BDOC availability is highest and redox conditions are rather oxic.[10,23,24] It is therefore reasonable to assume that removal rates of TrOCs may vary substantially along hyporheic flow paths, even if redox conditions are relatively similar. In previous investigations on the fate of TrOCs in the HZ, neither retardation nor the effect of benthic bio-layers and depth-dependent transport characteristics on the fate of TrOCs has been considered.[14,15,25] In addition, previous studies have mainly investigated the fate of parent TrOCs in the HZ,[14,15,25] while information on the fate of transformation products (TPs) such as guanylurea, the main TP of the antidiabetic drug metformin, valsartan acid, the main TP of compounds of the sartan group, or gabapentin-lactam a main TP of the anticonvulsant gabapentin in the HZ is widely lacking.

The objectives of the present study were to use concentration time series of TrOCs and conservative tracers sampled along a 40 cm long hyporheic flow path to calculate depth-dependent in-situ retardation coefficients and first-order removal rate constants of 28 TrOCs, including 7 transformation products, in the HZ of an urban lowland river in Berlin, Germany. We hypothesize that hyporheic reactivities of TrOCs are highest in the shallow HZ, where redox conditions are rather oxic and microbial activity is highest. We further anticipate that many TrOCs are retarded along hyporheic flow paths, which notably influences their residence times in the HZ and thus the estimation of hyporheic removal rates.

2. Methods

2.1 Site description and experimental overview

River Erpe, an urban lowland river located east of Berlin, Germany, receives 60% to 80% of its discharge from the municipal WWTP Münchehofe. The present study was conducted at Heidemühle (Lat: 52.478647, Long: 13.635146), a section of River Erpe that has been subject to previous investigations on the fate of TrOCs in the HZ due to its sandy streambed sediments.[14,15,26] Sediment characteristics at the sampling site were determined from one 40 cm long sediment core which was taken using a hand auger (inner diameter 9 cm) in close proximity of the sampling site (< 10 cm) and cut into 8 cm long sections, which were transferred into 5 KSAT rings (Meter, Germany) on site. Saturated hydraulic conductivity at 25 °C was measured using a KSAT device (Meter, Germany) and ranged between 1.6 x 10^{-5} m s^{-1} and 1.7 x 10^{-4} m s^{-1}. Porosity, determined from oven dried (105 °C, 48h) samples, decreased from 0.5 in the upper 8 cm of the HZ to 0.4 in the last 2 sub-cores (i.e. 24-40 cm depth).

The experimental setup consisted of three self-constructed mini-point samplers[26] (compare section 2.2) that were installed in the HZ in 10, 30 and 40 cm depth (Figure 1). An additional mini-point sampler was installed in the HZ in 20 cm depth. However, due to clogging, the sampler in 20 cm depth provided only a limited number of samples and was thus excluded from further analysis. To gain additional information on the hydrological conditions at the study site and to cross-check porewater velocities determined by conservative transport modeling (section 2.5), porewater velocities were additionally calculated from temperature time series in the HZ. To this end, a Multi-Level Temperature Stick[27] (MLTS, UIT, Dresden) was installed adjacent to the minipoint samplers (≈10 cm). Temperature time series were collected over the course of two weeks (14.06.-28.06.2016) in 5, 10, 15, 20, 30 and 50 cm depth in the HZ. Subsequently, vertical seepage fluxes and thermal dispersion coefficients were evaluated via the McCallum method[28] incorporated in the VFLUX 2.0 program.[29] The McCallum method simultaneously uses phase shifts ($\Delta\varphi$) and amplitude damping ratios (A_r) of two sinusoidal temperature time series to calculate both the thermal dispersivity and the Darcy velocity via an analytical solution of the one-

dimensional heat transport equation. In VFLUX, dynamic harmonic regression,[30] a form of harmonic regression in which the spectral coefficients describing a periodic signal can be non-stationary, is used to estimate phase and amplitude information from the measured time series. Vertical seepage fluxes and thermal dispersion coefficients were calculated from measured temperature time series in 5 and 10 cm, 10 and 30 cm and 20 and 50 cm depth in the HZ, yielding parameter estimates at center-of-pair depths of 7.5 cm, 20 cm and 35 cm, respectively, covering the three different model sections in the HZ (compare section 2.5). Further details on the method and its underlying assumptions can be found elsewhere[14,26] and in the Supporting Information (SI, section SI-01).

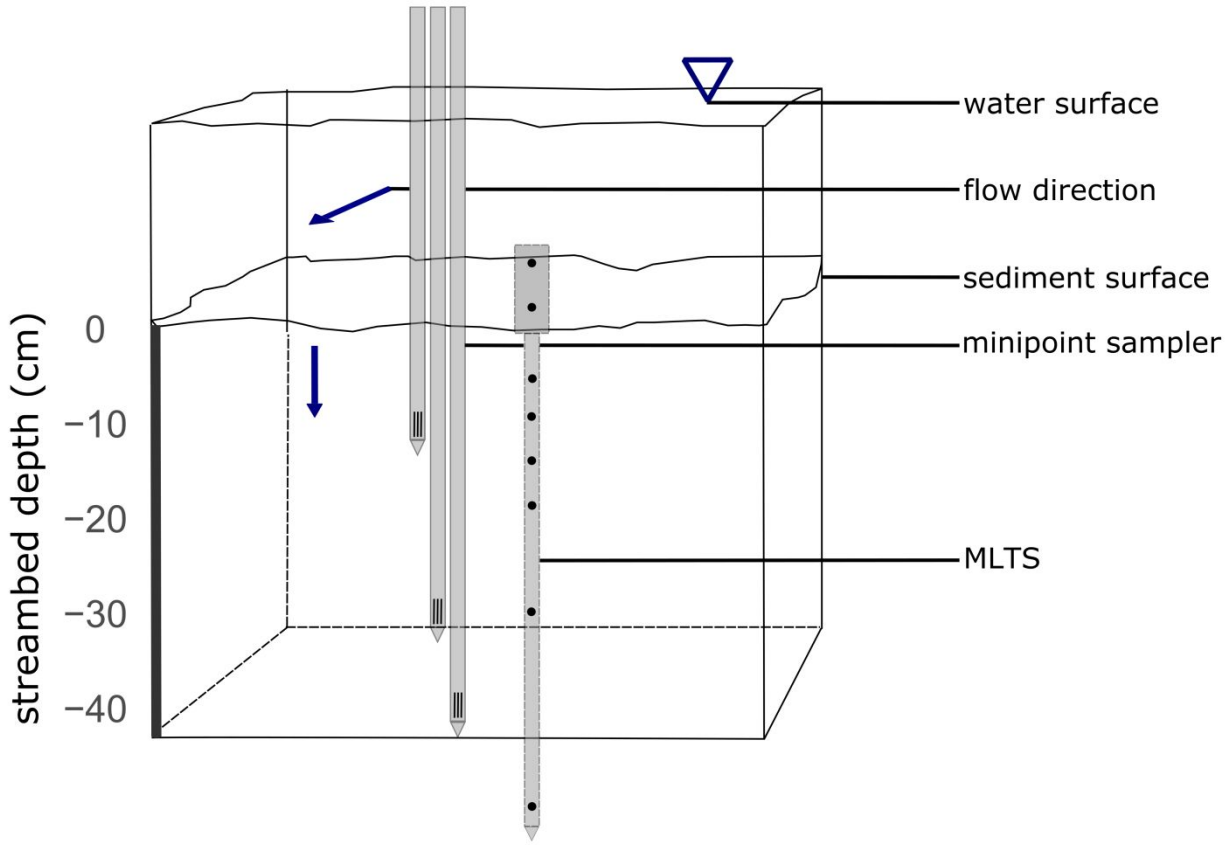


Figure 1 Experimental setup showing the three minipoint sampler installed in 10 cm, 30 cm and 40 cm depth in the hyporheic zone (HZ). The samplers were installed in a line (< 1 cm distance) perpendicular to the water flow direction. A Multilevel Temperature Stick (MLTS) was installed in close proximity (≈ 10 cm) next to the minipoint sampler array. Blue arrows indicate surface water and predominant hyporheic flow directions. Minipoint samplers were sampled from an aluminum bridge spanning the river channel (not shown).

117 **2.2 Water sampling**

118 Hyporheic porewater samples were collected hourly between 22:30 on June, 15th and 15:30 on June 16th
119 2016 using self-constructed mini-point samplers.[26] In brief, the mini-points consisted of HPLC tubes
120 (PEEK, ID 0.03 inch, Sigma Aldrich, USA) that were inserted into 1.5 m long stainless steel tubes (ID 0.7
121 mm). At the tip of the steel tubes, four 1-cm long laser cut slits (< 0.1 mm) allowed water flow but acted
122 as a filter screen for most sediment particles. The HPLC tubes were connected to a syringe pump (NE-
123 1600 New Era Pump Systems, Inc, Farmingdale, USA) via Swagelok fittings (Swagelok, USA) to allow
124 slow, constant pumping of hyporheic porewater. Thirteen ml of hyporheic porewater were sampled
125 applying a constant sampling rate of 1 ml min^{-1}. In previous investigations conducted at the same site
126 pumping rates of 1 ml min^{-1} have been found to be sufficiently low to maintain the integrity of the
127 hyporheic flow field.[26] Electrical conductivity (EC) was measured in each sample and in the surface water
128 using handheld EC meters (GMH 3431, Greisinger, Germany). Every four hours, pH was measured in the
129 hyporheic porewater samples and in the surface water using a handheld pH meter (SenTix 41, WTW,
130 Germany), calibrated prior to sampling. Samples in the HZ were related to surface water samples,
131 obtained from an automatic water sampler (model 3700, Teflon suction line, Teledyne ISCO, Lincoln,
132 NE.) located 150 m upstream of the sampling site following procedures described elsewhere.[31] Samples
133 for TrOC and dissolved organic carbon (DOC) analysis were filtered through regenerated cellulose
134 syringe filters (0.2 µm, Macherey-Nagel, Germany) and stored in amber glass bottles with Teflon lined
135 caps. Samples for TrOC analysis were immediately frozen on site. Samples for DOC analysis were stored
136 at 4° C in the dark and were measured within two weeks after sampling. Samples for NO_3^--N and major
137 cation analysis were filtered through cellulose acetate syringe filters (0.2 µm, Sartorius, Germany) and
138 stored in polyethylene bottles at 4 °C until analysis. Samples for total dissolved iron and dissolved
139 manganese analysis were additionally acidified to pH ≈ 2.0 using HCl. A sampling period of 17 h was
140 considered sufficient as the aim of the present study was to investigate TrOC reactivity and the effect of
141 retardation on TrOC transport along a relatively constrained hyporheic flow path. From previous studies at

142 the same field site it was known that (i) chemical conditions in River Erpe oscillate on a daily basis
143 (concentration troughs in the morning, peaks in the afternoon) but are relatively constant over the course
144 of weeks and (ii) that porewater velocities were in the order of several cm per hour.[14,31]
145

146 **2.3 Analytical procedures**

147 To enlarge the number of target compounds, samples were split and analyzed in parallel using high
148 performance liquid chromatography with tandem mass spectrometry (HPLC-MS/MS) at the Department
149 of Environmental Science and Analytical Chemistry (ACES) at Stockholm University and the Chair of
150 Water Quality Engineering at Technical University of Berlin (TUB) following standard protocols
151 established previously.[26,32,33] In brief, separation of TrOCs was achieved via a XSelect HSS T3 HPLC
152 column (2.5 µm particle size, 2.1 * 50 mm, Waters, USA) at TUB and an Acquity UPLC HSS T3 column
153 (1.8 µm, 2.1 mm × 100 mm, Waters, USA) at ACES. Both protocols used linear gradients (ultra-pure
154 water versus 100% methanol; HPLC grade, J.T. Baker, USA). A TSQ Vantage (Thermo Fisher Scientific,
155 USA) and a Quantiva triple-quadrupole mass spectrometer in ESI ± modes were used for MS/MS analysis
156 at TUB and ACES, respectively. In both methods, TrOC were identified based on the characteristic ratio
157 of two ion fragments and quantified via isotope-substituted standards (Toronto Research Chemicals,
158 Canada) in combination with the most abundant fragment ion (Table SI-01). In both methods, a series of
159 calibration standards was measured before and after each sampling sequence. To assess analytical errors,
160 samples at TUB were measured in triplicate, while at ACES quality control standards were measured
161 during each run. In total, 29 TrOCs, including 22 parent compounds (PCs) and 7 transformation products
162 (TPs), were analyzed in the present study. Ultra-pure water (Maxima UF device, ELGA LabWater,
163 Germany) and tap water were measured as method blank at TUB and ACES, respectively. Limits of
164 detection (LODs) and quantification (LOQs) for each target compound and additional information on the
165 analytical procedures and data evaluation are provided in the SI (section 2). Concentrations of major
166 cations and total dissolved iron and manganese were measured using inductively coupled plasma optical
167 emission spectrometry (ICP-OES, ICP iCAP 6000series, Thermo Fisher). Nitrate-N concentrations were
168 measured via continuous-flow-analysis (SAN ++, Skalar) following DIN EN ISO 13395.
169 Absorbance spectra of dissolved organic matter (DOM, 250–600 nm, every 5 nm) and excitation-emission
170 matrices (EEMs, excitation wavelength ranging from 250 to 600 nm, 5 nm increments; emission range of

250–550 nm 1.64 nm increments) were measured in triplicate at a Horiba Aqualog (Horiba Ltd, Japan) in a 1 cm quartz cuvette. One blank (MiliQ water) was measured for every 9 measurements. Scan speed was 12 000 nm min^{-1} at a response time of 0.01 s. The Humification Index (HIX), a measure of the degree of humification of DOM,[34] was calculated after EEMs were blank-subtracted and corrected for the inner filter effect. DOC concentration was measured in triplicate at a varioTOC cube (elementar Analysensysteme, Germany). Specific UV absorbance at 254 nm ($SUVA_{254}$) was calculated by normalizing the decadal absorbance measured at 254 nm to DOC concentration (mg/L).[35]

2.4 Calculation of relative removal percentages

To assess overall TrOC removal along the investigated hyporheic flow path and to cross-validate calculated removal rate constants (section 2.5), relative TrOC removals were calculated between the surface water and hyporheic water in 40 cm depth and between other pairs of concentration time series, i.e., between the surface water and hyporheic water in 10 cm depth, between hyporheic water in 10 and in 30 cm depth and between hyporheic water in 30 and in 40 cm depth. Because measured concentrations varied with time, relative removal of a given TrOC (x) between two sampling depths (Rel_x) was calculated using cumulative concentrations of a TrOC normalized to cumulative concentrations of a stable reference compound:[36,37]

$$\mathrm{Rel}_x^{in-out} = \left(1 - \frac{\sum_i^n c_{x,out,i} \sum_i^n c_{ref,in,i}}{\sum_i^n c_{x,in,i} \sum_i^n c_{ref,out,i}}\right) x\ 100\% \quad (1)$$

whereby $c_{x,in}$ and $c_{x,out}$ ($c_{ref,in}$ and $c_{ref,out}$) are the concentrations of the upper and lower concentration time series of a TrOC (a stable reference compound), respectively, and n is the number of data points in each time series. In the present study we used *O*-desmethylvenlafaxine (MLX) as a stable reference compound as it showed low retardation along the hyporheic flow path and was found to be rather stable in the HZ (compare section 3.3). The approach was cross-validated using the diurnal varying EC signal measured in

193 the surface water and in hyporheic porewater samples as another conservative reference (SI section 4).
194 Removal of a TrOC was considered significant if the 95% confidence interval of the relative removal,
195 computed using the respective analytical uncertainties of each TrOC (Table SI-02), did not include zero.
196 The applicability of equation 1 requires either relatively constant flow conditions or a positive correlation
197 between the reference compound and the target TrOC concentrations. Both requirements were likely met
198 in the present study as the study site was characterized by strong downwelling conditions (compare
199 section 3.1) and concentrations of TrOCs (with the exception of acesulfame, metoprolol acid and
200 metformin) were well correlated to *O*-desmethylvenlafaxine concentrations (Pearson Product Moment
201 Correlation coefficients > 0.7, p-value < 0.05). Equation 1 is based on the assumption that the transport
202 time scales of both, the target TrOC and the reference compound, are similar. Thus Rel_x calculated for
203 strongly retarding TrOCs (compare section 3.4) should be treated with caution.
204

205 **2.5 Reactive transport modeling**

206 Measured concentration time series in the HZ were evaluated using the one-dimensional (1D) advection-
207 dispersion transport equation including first-order degradation and retardation (1D-ADE). Assuming
208 steady and uniform flow in a homogeneous medium, and time invariant dispersion, retardation and first-
209 order decay the 1D-ADE equation can be written as:

$$R\frac{\partial c}{\partial t} = D_h\frac{\partial^2 c}{\partial x^2} - v\frac{\partial c}{\partial x} - \lambda c \quad (2)$$

210 where c denotes the concentration of a (reactive) compound, D_h the effective hydrodynamic dispersion
211 coefficient ($m^2\ h^{-1}$), v the vertical porewater velocity ($m\ h^{-1}$), λ a first-order removal rate constant (h^{-1}) and
212 R the retardation coefficient (-). Equation 2 was implemented in the programming language Python and
213 solved numerically using a finite-difference scheme. The HZ was vertically divided into three sections
214 delimited by each pair of concentration time series: Section 1 between the surface water and 10 cm depth,
215 section 2 between 10 and 30 cm depth and section 3 between 30 and 40 cm depth. For each section in the
216 HZ, equation 2 was solved separately, yielding independent parameter estimates for each section. The
217 upper concentration time series served as an upper boundary condition in equation 2. The lower boundary
218 condition (in 100, 110 and 120 cm depth for sections 1, 2 and 3, respectively) was set to zero. The lower
219 concentration time series in each section was used for parameter estimation.
220 Parameter estimation was achieved using the DREAM algorithm,[38,39] a Bayesian parameter optimization
221 method which employs evolutionary Monte Carlo Markov chains to estimate posterior probability density
222 distributions (posteriors) of model parameters. In a first step, posteriors of conservative transport
223 characteristics (i.e. v and D_h) were estimated from EC time series by setting λ to zero and R to unity. In a
224 second step, measured concentrations of TrOCs, DOC and NO_3^--N were used to derive first-order removal
225 rate constants and, for TrOCs, retardation coefficients using the previously derived posteriors for v and D_h
226 as priors. This approach was justified as the relative contribution of molecular diffusion to D_h, which at
227 sediment-water interface is commonly described as the sum of molecular, hydrodynamic and turbulent

diffusivities,[40,41] can be considered negligible, because porewater velocities measured in the present study were larger than 10^{-6} m s^{-1} (compare section 3.1) and molecular diffusion coefficients (D_{mol}) for the investigated TrOCs are generally smaller than 10^{-9} m^2 s^{-1} (Table SI-03, see SI section 3.3 for details on calculation of D_{mol}).

Retardation coefficients can only be estimated from measured concentration time series that show a distinct, traceable temporal pattern, i.e., a trough or peak. For TrOCs, parameter optimization via DREAM was therefore conducted using two models, one including ($R \geq 1$) and one excluding the effect of retardation (R=1). If retardation coefficients could not be estimated, i.e., if posteriors of R were indifferent from their priors, λ was estimated from the model in which R was set to unity. The conceptual model of equation 2 assumes that i) water flows vertically from the surface into the HZ and that ii) mixing with groundwater can be neglected. These assumptions were justified as i) the study site was characterized by strong downwelling conditions (compare section 3.1) and a previous investigation on hyporheic flow fields at the same site found that horizontal flow components were of minor importance[14] and ii) relative removal of *O*-desmethylvenlafaxine, a stable reference compound (compare section 2.4), was calculated to be -3 to 4% (Table 2) indicating that groundwater input along the investigated flow path was negligible. Details on the numerical scheme used to solve equation 2 and the parameter estimation procedure including the prior distributions of model parameters and other DREAM settings are provided in the SI.

3. Results & Discussion

3.1 Transport characteristics in the hyporheic zone

Median porewater velocities, estimated from temperature depth profiles using VFLUX, ranged between 0.06 and 0.11 m h^{-1} (Table 1). These strong downwelling conditions (positive flux = downward flow) are in line with values reported previously for the same study site.[14] As a result of low WWTP discharge during nighttime, EC time series in the surface water of River Erpe follow a saw-toothed pattern with distinct EC troughs in early morning hours.[14] The EC trough, measured in the surface water between 02:00

and 10:00 on June 16th propagated into the HZ and served as a natural tracer from which conservative transport parameters were modeled using equation 2 (Figure 2). Porewater velocities derived from EC time series using the 1D-ADE model ranged from 0.07 m h^{-1} to 0.17 m h^{-1} and are thus somewhat higher than porewater velocities calculated from temperature time series using VFLUX, particularly in the upper two sections of the HZ (Table 1). Differences in porewater velocities might be the result of erroneous VFLUX calculations (e.g., due to violations of VFLUX model assumptions) and sediment heterogeneity. Values for the effective hydrodynamic dispersion coefficient (D_h) ranged between 10 x 10^{-4} and 48 x 10^{-4} m^2 h^{-1} and are within the same order of magnitude as values of the effective thermal dispersion coefficient calculated by VFLUX (D_t, Table 1).

Table 1 Mean values (± 1 standard deviation) of porewater velocities (v) and dispersion coefficients (hydrodynamic dispersion coefficient D_h, thermal dispersion coefficient D_t) derived from i) electrical conductivity (EC) time series using eqn. 2 (1D-ADE) and ii) from temperature time series using VFLUX 2.0 for all three sections in the hyporheic zone. In addition, removal rates of NO_3^--N ($k_{nit\text{-}N}$) and DOC (k_{DOC}) are shown.

depth	1D-ADE		VFLUX 2.0		NO_3^--N	DOC
	v	D_h	v	D_t	$k_{nit\text{-}N}$	k_{DOC}
cm	m h^{-1}	m^2 h^{-1} x 10^{-4}	m h^{-1}	m^2 h^{-1} x 10^{-4}	h^{-1}	h^{-1}
0-10	0.14 ± 0.01	48 ± 6	0.11 ± 0.02	73 ± 05	0.60 ± 0.03	0.30 ± 0.01
10-30	0.17 ± 0.01	10 ± 3	0.07 ± 0.01	34 ± 01	0.10 ± 0.01	0.12 ± 0.01
30-40	0.07 ± 0.01	46 ± 12	0.06 ± 0.01	36 ± 01	1.25 ± 0.03	0.05 ± 0.01

3.2 Redox zonation and DOC dynamics in the hyporheic zone

DOC concentrations gradually decreased along the investigated hyporheic flow path, while $SUVA_{254}$ and HIX, measures of the aromaticity and the degree of humification of DOC, respectively increased (Figure SI-04). A general decrease of DOC concentrations and an increase of $SUVA_{254}$ along hyporheic flow paths has been reported previously[42] and was attributed to preferred degradation of non-aromatic, biodegradable DOC fractions in the HZ. The largest removal rate of DOC as well as the largest change in HIX occurred between 0 and 10 cm depth (Table 1, Figure SI-04), suggesting that the largest change in DOC quantity and quality along the investigated hyporheic flow path occurred in the upper 10 cm of the HZ. This finding is in agreement with previous investigations in the HZ, suggesting that the highest carbon turnover rates in the HZ are typically found within the first cm of the HZ in the so called active benthic bio-layer.[10] A more detailed discussion of DOC dynamics in the HZ including information on other EEM indices is provided in the SI (SI section 6).

During the sampling period, nitrate concentrations in the surface water were high (median concentrations 7.0 mg/L NO_3^--N, Table SI-04). In the HZ, nitrate removal rates were high between 0 and 10 cm depth, low between 10 and 30 cm depth and highest between 30 and 40 cm depth (Figure SI-03, Table 1). Concentrations of total dissolved iron and dissolved manganese in the HZ were relatively low (< 0.05 mg/L, Table SI-04), indicating the redox conditions in the stream sediment were not yet within iron- and manganese-reducing ranges. Removal of nitrate-N in the HZ can be caused by microbial uptake (i.e., assimilation) and denitrification occurring in both anoxic sections of the HZ and in anoxic microzones.[42–44] Because DOC removal rates were highest in the shallow HZ, it is reasonable to assume that in addition to potential denitrification in anoxic microzones,[23] nitrate-N removal in the upper 10 cm in the HZ was primarily caused by biotic assimilation. The higher nitrate-N removal rate in the deeper HZ (i.e., between 30 and 40 cm depth), however, is presumably attributable to denitrification. It is therefore likely that redox conditions in the bulk porewater were rather oxic in the first 30 cm of the HZ and became suboxic (i.e. denitrifying) thereafter. Redox zonation in the HZ is a function of biogeochemical parameters, such as

292 microbial turnover rates and the abundance and quality of electron acceptors and donors, physical
293 parameters such as temperature and transport characteristics that control residence time distributions in the
294 HZ. Compared to earlier investigations on redox zonation in the HZ at the same study site,[14] redox
295 zonation in the present study was shifted downwards (i.e. deeper onset of denitrification and
296 iron/manganese reduction). In line with previous studies,[23] we attribute this finding to larger porewater
297 velocities measured in the present study.
298

3.3 Reactivity of trace organic compounds in the HZ

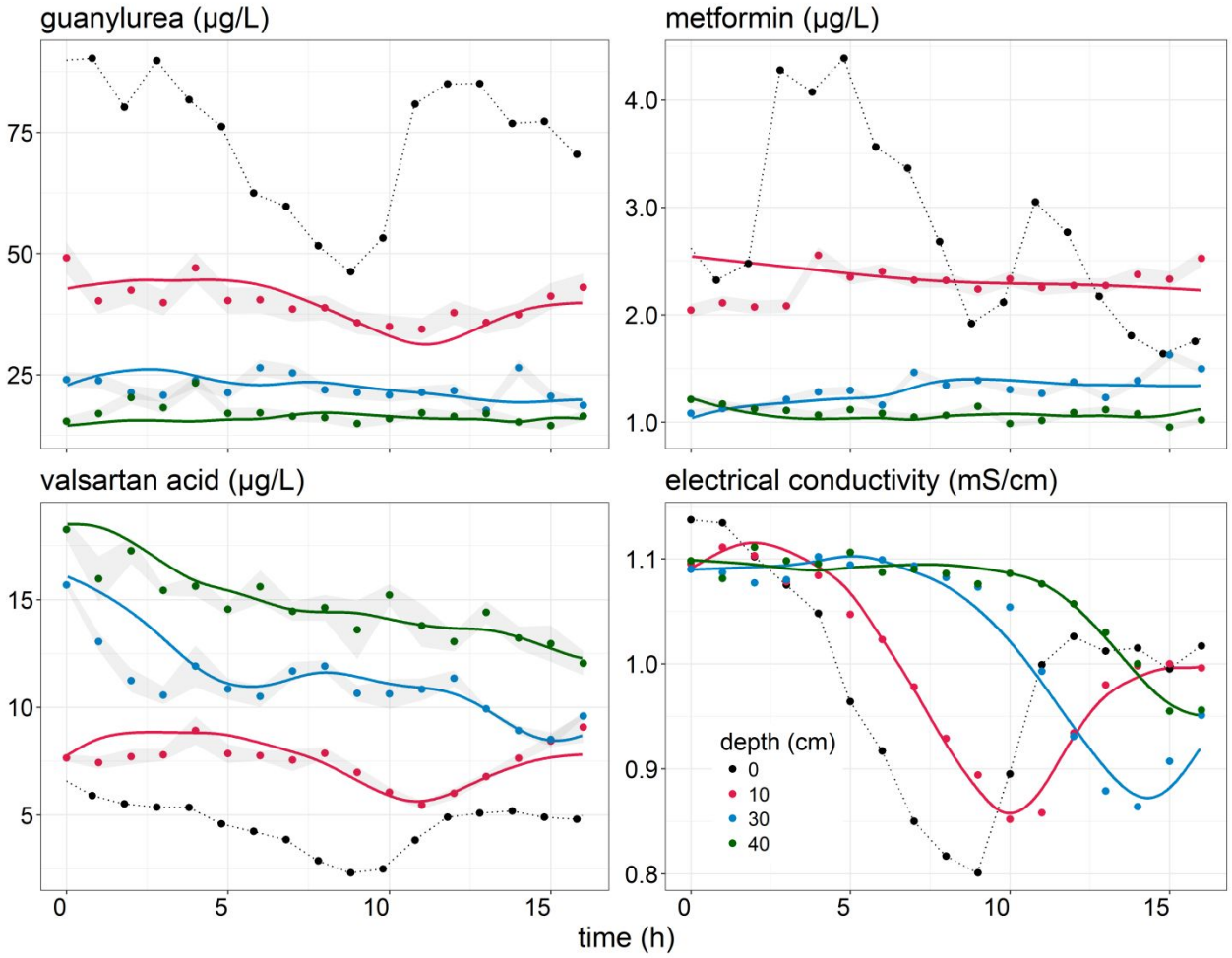
Out of the 29 investigated TrOCs, relative removals (%) and first-order removal rates could be calculated from measured concentration time series of 28 compounds (Table 2). For epoxy-carbamazepine (EBZ), concentrations were either below LOQ or just slightly above LOQ and thus EBZ was not considered in further analysis (Table SI-04). Modeled and measured concentration time series for valsartan acid (VSA), metformin (MEF) and its TP guanylurea (GUA) and EC are depicted in Figure 2. Measured and modeled concentration time series of the remaining TrOCs are shown in Figures SI 05-32. Twenty-two compounds were significantly removed between the surface water and 40 cm depth with half-lives within the first 10 cm of the HZ ranging between 0.1±0.01 h for iopromide and 3.5±0.3 h for tramadol (Table 2).

The highest removal rate constants were calculated for the iodinated X-ray contrast agents iomeprol (IOM) and iopromide (IOP). Complete de-iodination of both compounds in saturated sediments has only been observed under anoxic redox conditions[45] but both compounds are known to readily loose side chains of the iodinated ring structure under aerobic conditions.[46,47] It is therefore likely that the high removal rates calculated in the present study are due to transformation of both compounds and do not represent complete mineralization. Removal of the artificial sweetener acesulfame (ACS), the lipid-lowering agent bezafibrate (BZF), the anti-corrosive agents benzotriazole and methylbenzotriazole and the anticonvulsant GAB along oxic to suboxic (i.e. denitrifying) flow paths in hyporheic sediments has previously been described in laboratory column experiments[12,48] and observed in the HZ.[14] For ACS, reported half-lives range from 1.2[14] to 5[12] h and for BZF and GAB were calculated to be 1.2 h and 0.96 h in a previous investigation at the same site.[14] Thus, half-lives for ACS, BZF and GAB calculated in the present study match half-lives calculated previously for hyporheic sediments. Removal of gabapentin-lactam, a major TP of GAB,[48] in saturated sediments has previously been reported during bank filtration, with half-lives between 1.2 and 3.7 h.[49] These values match the ones calculated for the first 10 cm of the HZ (2.3±0.2 h), although no further removal of GPL was observed in deeper section of the HZ.

Although the antidiabetic drug metformin and its main TP guanylurea[50] have been detected ubiquitously in surface waters,[51,52] qualitative information on the fate of the two compounds in saturated sediments is relatively scarce. Both were found to be rather stable in laboratory batch experiments;[50,53] a finding that cannot be confirmed in the present study where they show half-lives in the HZ of several hours. Calculated half-lives for the beta-blockers MTP are in line with findings of a laboratory column study reporting half-lives of several hours for oxic/suboxic conditions,[12] but contrast results of investigations conducted previously at the same study site, in which MTP was, on average, not significantly removed along a 20 cm long hyporheic flow path.[14] Metoprolol acid (MTA), a main TP of MTP, was formed in the HZ, suggesting that removal of MTP in the HZ is at least in part due to transformation into MTA. Quantitative information on the fate of the beta blocker sotalol (SOT) and the opioid analgesic tramadol (TRA) in the HZ is limited. For SOT and TRA, a concentration decrease in the HZ[25] and in sediments of a flume study mimicking the HZ,[13] respectively, has been reported, but no removal rates were calculated. The antihypertensive drugs olmesartan (OLM), irbesartan (IRB), candesartan (CAN) and valsartan (VAL) were significantly removed along the investigated flow path. Simultaneously concentrations of their common TP valsartan acid[54,55] (VSA) increased. At least part of the removal of OLM, CAN, VAL and IRB can therefore be attributed to transformation to VSA. While VAL removal in hyporheic sediments has been described,[17] OLM and CAN were found to be rather stable in both, hyporheic sediments and during river bank filtration.[17,49] Although removal of VSA has been described in bank filtration systems,[49] concentrations of its PCs were likely too high in the HZ and thus net formation rates were higher than potential VSA removal rates.

Carbamazepine (CBZ) and one of its TPs dihydroxy-carbamazepine (DBZ), diclofenac (DCF), diatrizoic acid (diatrizoate, DTA) and venlafaxine (VLX) and its TP *O*-desmethylvenlafaxine (MLX) were not significantly removed and were thus considered to be rather stable along the investigated flow path (Table 2). CBZ is well known for its stability in saturated sediments[56] and hitherto, removal has only been observed under iron-reducing conditions after long (several days) residence times.[57] Since concentrations

348 of DBZ remained relatively constant along the investigated flow path it is reasonable to assume that
349 transformation of CBZ to DBZ along short (<40 cm) and rather oxic flow paths in the HZ is limited.
350 Laboratory and field studies have demonstrated that VLX,[58] DCF[12,14] and DTA[59] can be removed in
351 saturated sediments. It is therefore likely that in the present study exposure times to favorable
352 biogeochemical conditions in the HZ times were likely too short to facilitate significant removal of these
353 compounds.
354 The anticonvulsant primidone (PRI) and the antibiotic sulfamethoxazole (SMX) showed negative removal
355 indicating a concentration increase in the HZ. To the best of our knowledge, formation of PRI in the HZ
356 has not been reported and we thus attribute the small concentration increase (18±7%) to desorption
357 processes. For SMX however, back-transformation of photo-transformation products into SMX has been
358 observed in water/sediment systems.[60] It is therefore perceivable that back-transformation was responsible
359 for the observed concentration increase of SMX. The TrOC 4-formylaminoantipyrin (FAA), a human
360 metabolite of metamizole[61] (a phenazone-type analgesics not investigated in the present study), was found
361 to be removed between 0 and 30 cm depth but was formed between 30 and 40 cm depth. Removal of FAA
362 in oxic sections of saturated sediments has been described,[12,62] although a previous investigation at the
363 same site found inconsistent behavior (removal in some profiles, formation in others) of the compound.[14]
364 It remains unclear whether the formation of FAA during suboxic (i.e. denitrifying) redox conditions is due
365 to back-transformation or due to increased transformation of its PC(s).
366 For some compounds (e.g. OLM), modeled concentration time series could be fitted well over the entire
367 time series. For other compounds such as MTP, VSA or GUA (Figure 1, Figure SI-24), modeled
368 concentrations matched measured concentration time series well in some parts of the time series but
369 deviated in others. Such discrepancies indicate that model assumptions such as time invariant porewater
370 velocities or removal rate constants were not met throughout the sampling event. Time varying removal
371 rate constants could be the consequence of temperature dependent biotransformation rates or varying
372 substrate and TrOC concentrations in the surface water.



373

374 **Figure 2** Measured (dots) and modeled (solid lines) concentration time series in 10 cm, 30 cm and 40 cm depth in the hyporheic
375 zone (HZ) and measured concentration time series in the surface water (0 cm) of guanylurea (GUA), metformin (MEF), valsartan
376 acid (VSA) and electrical conductivity (EC). For concentration time series measured in the HZ, analytical uncertainty (one
377 standard deviation) is shown in grey. Note that for modeling purposes, concentration time series in the surface water were linearly
378 interpolated (black dashed line) and that for EC no measurement uncertainties were available.

379

Table 2 Relative removal in the upper 40 cm of the hyporheic zone (Rel_x^{0-40}, %), half-lives ($t_{1/2}$, h) and retardation coefficients (R, dimensionless) of all trace organic compounds investigated in the present study except epoxy-carbamazepine calculated between 0 and 10, 10 and 30 and 30 and 40 cm depth in the hyporheic zone. Note that retardation coefficients could only be estimated from input time series that showed a distinct temporal pattern, i.e. a trough or peak. Half-lives exceeding the sampling period (i.e., 17 h) were set to infinity.

TrOC	Rel_x^{0-40} (%)	$t_{1/2}$ (h)			R (-)		
	0-40	0-10	10-30	30-40	0-10	10-30	30-40
acesulfame (ACS)	78±1	0.5±0.0	2.9±0.2	0.9±0.0	1.2±0.1	1.0	n.e.
benzotriazole (BTA)	63±2	0.9±0.0	2.6±0.1	12.6±2.6*	4.0±0.5	n.e.	n.e.
bezafibrate (BZF)	69±2	0.8±0.0	3.7±0.1	1.9±0.2	2.6±0.3	2.8±0.0	n.e.
candesartan (CAN)	27±4	1.1±0.1	12.9±3.8[f,*]	inf	1.7±0.2	1.3±0.1	n.e.
carbamazepine (CBZ)	9±5*	9.8±1.6	inf	inf	3.6±0.3	n.e.	n.e.
dihydroxy-carbamazepine (DBZ)	-1±6*	3.2±0.4*	11.4±5.3	15.8±8.9[f]	2.2±0.3	n.e.	n.e.
diclofenac (DCF)	-11±6*	inf	inf	inf	4.3±0.3	n.e.	n.e.
diatrizoic acid (DTA)	0±9*	6.3±1.4*	inf	inf	1.1±0.1	2.0±2.5	n.e.
4-formylaminoantipyrine (FAA)	10±4	1.2±0.1	inf	9.4±0.9[f]	2.4±0.2	1.5±0.1	n.e.
gabapentin (GAB)	79±1	0.4±0.0	1.5±0.0	2.1±0.1	1.4±0.0	1.4±0.1	3.7±0.6
gabapentin-lactam (GPL)	12±5	2.3±0.2	8.9±1.4[f,*]	inf	1.3±0.2	n.e.	n.e.
guanylurea (GUA)	78±1	0.6±0.0	1.4±0.0	2.8±0.3	2.6±0.2	n.e.	n.e.
iomeprol (IOM)	98±0	0.1±0.0	0.7±0.0	0.7±0.1	1.9±0.4	1.1±0.1	n.e.
iopromid (IOP)	98±0	0.1±0.0	0.8±0.1	0.6±0.3	n.e.	n.e.	n.e.
irbesartan (IRB)	37±3	1.0±0.0	7.1±1.3[f]	3.9±0.6	3.5±0.1	n.e.	n.e.
methylbenzotriazole (MBT)	36±3	1.7±0.0	4.1±0.1	11.6±0.9[f]	3.3±0.1	n.e.	n.e.
metformin (MEF)	66±2	1.1±0.1	1.6±0.0	3.9±0.2	15.3±2.2	n.e.	n.e.
O-desmethylvenlafaxine (MLX)	0±6*	14.1±6.8[f]	12.1±5.6*	inf	1.5±0.2	n.e.	n.e.
metoprolol acid (MTA)	-35±8	2.0±0.2[f]	12.8±4.7[f,*]	inf	n.e.	n.e.	n.e.
metoprolol (MTP)	90±1	0.2±0.0	1.3±0.1	2.5±0.5	4.5±0.5	n.e.	n.e.
olmesartan (OLM)	18±4	1.5±0.1	inf	inf	1.4±0.1	1.3±0.2	n.e.
primidone (PRI)	-18±7	10.3±3.9[f,*]	inf	11.0±0.8[f,*]	1.4±0.1	n.e.	n.e.
sulfamethoxazole (SMX)	-47±8	6.8±1.4[f,*]	4.9±0.4[f]	11.1±1.7[f,*]	1.6±0.2	1.1±0.1	1.1±0.1
sotalol (SOT)	50±2	0.8±0.0	3.3±0.2	5.8±0.6*	1.9±0.2	n.e.	n.e.
tramadol (TRA)	12±4	3.5±0.2	inf	inf	2.2±0.2	n.e.	n.e.
valsartan (VAL)	26±4	1.1±0.0	7.8±0.2	9.4±1.1[f,*]	1.9±0.0	n.e.	n.e.
venlafaxine (VLX)	-5±9*	6.2±2.2*	inf	9.0±5.8*	3.6±0.6	n.e.	n.e.
valsartan acid (VSA)	-205±15	1.2±0.0[f]	2.4±0.1[f]	7.6±0.9[f]	1.1±0.1	1.0±0.0	n.e.

inf = half-life > 17 h. * = not significantly removed/formed as indicated by Rel_x. n.e. = not estimated. f = TrOC formation.

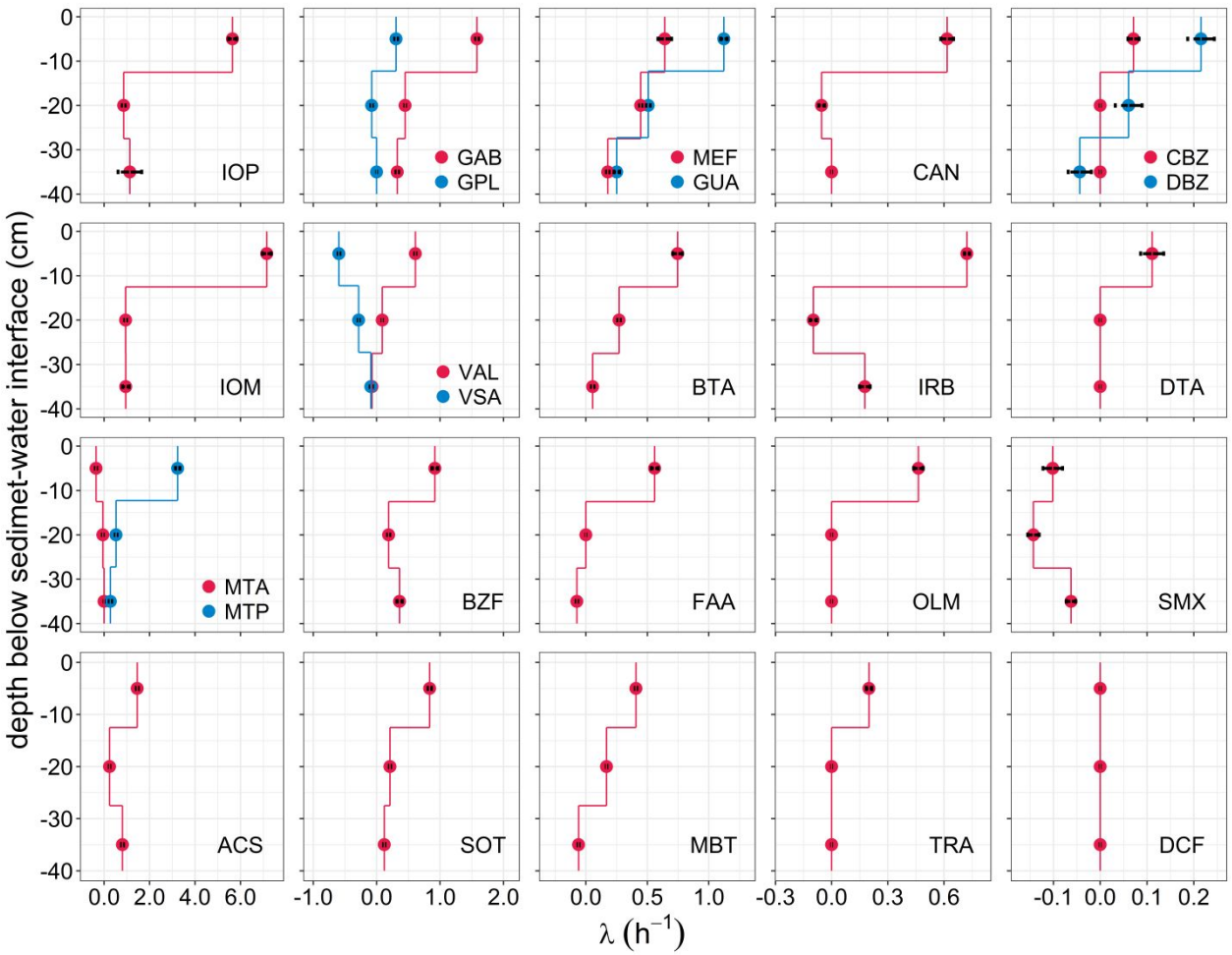


Figure 3 First-order removal rate constants (λ) as a function of depth of all investigated parent compounds (PCs, shown in red) and transformation compounds (TPs, shown in blue) except, primidone, epoxy-carbamazepine, venlafaxine and *O*-desmethylvenlafaxine. Error bars indicate one standard deviation. ACS, acesulfame; BTA, benzotriazole; BZF, bezafibrate; CAN, candesartan; CBZ, carbamazepine; DBZ, dihydroxy-carbamazepine; DCF, diclofenac; DTA, diatrizoic acid; FAA, 4-formylaminoantipyrine; GAB, gabapentin; GPL, gabapentin-lactam; GUA, guanylurea; IOM, iomeprol; IOP, iopromide; IRB, irbesartan; MBT, methylbenzotriazole; MEF, metformin; MTA, metoprolol acid; MTP, metoprolol; olmesartan, OLM; SMX, sulfamethoxazole; SOT, sotalol; TRA, tramadol; VAL, valsartan; VSA, valsartan acid.

395 **3.4 Retardation of TrOCs in the HZ**

396 Surface water concentration time series of all 28 TrOCs that were further investigated in the present study
397 showed a pronounced temporal pattern (i.e. a concentration trough) and thus retardation coefficients for all
398 TrOCs except IOP and MTA could be calculated for the first 10 cm in the HZ. However, concentration
399 time series of many TrOCs measured in 10 and 30 cm did no longer exhibit a distinct temporal pattern and
400 thus retardation coefficients could not be estimated between 10 - 30 and 30 - 40 cm for these compounds
401 (Table 2). Calculated retardation coefficients ranged from 1.1±0.1 (i.e., no retardation) for compounds
402 such as ACS, VSA, and DTA to 15.3±2.2 for MEF (Table 2).
403 Retardation of TrOCs along hyporheic flow paths is due to reversible sorption processes caused by a
404 variety of interaction mechanisms between TrOCs and streambed sediments and biofilms. Neutral TrOCs
405 interact with streambed materials predominately via hydrophobic partitioning, while sorption and
406 retardation of ionizable compounds can additionally be caused by electrostatic interactions and surface
407 complexation.[18] At ambient pH values measured in River Erpe during the sampling campaign (pH ≈ 7.3),
408 7 of the investigated compounds occur as cations (GUA, MEF, MTP, SOT, VLX, MLX and TRA), 10
409 TrOCs occur as anions (ACS, BZF, CAN, DCF, DTA, IRB, OLM, SMX, VAL and VSA), 2 occur as a
410 zwitterions (GAB, MTA) and 9 do not carry any charge (BTA, CBZ, DBZ, FAA, GPL, IOM, IOP, MBT,
411 and PRI). To assess the possible influence of hydrophobic partitioning retardation, Pearson Product
412 Moment correlations were calculated between retardation coefficients estimated for the first 10 cm in the
413 HZ and pH-dependent octanol-water partitioning coefficients ($logD_{ow}$) of the respective TrOCs (obtained
414 from www.chemicalize.com, Table SI-05). Retardation coefficients of positively charged TrOCs were all
415 larger than 1 and did not significantly correlate with $logD_{ow}$ values (Table SI-06), suggesting that the
416 contribution of hydrophobic partitioning to retardation of cationic TrOCs is negligible. This finding is in
417 line with previous observations indicating that sorption of cationic TrOCs, such as MEF, its TP GUA,[63]
418 VLX[64] and beta-blockers such as MTP and SOT[13,65] to sediment materials can be substantial and occurs
419 predominately via electrostatic interactions. By contrast, $logD_{ow}$ values of negatively charged TrOCs

420 correlated positively with estimated retardation coefficients (Table SI-06), indicating that retardation of
421 anionic TrOCs in the HZ is at least partially caused by hydrophobic partitioning into sediment organic
422 matter. This finding is in agreement with work that showed that sorption of anionic compounds is driven
423 by their hydrophobicity rather than by electrostatic interactions.[66] For the neutral TrOCs PRI, CBZ, and
424 DBZ, retardation coefficients found in a laboratory column (R_{CBZ} = 2.1, R_{DBZ} = 3.2, f_{oc} = 0.29%)[20] and
425 batch tests (R_{CBZ} = 3.6-5.3, R_{PRI} = 1.2, f_{oc} = 0.23%)[21] compared well to values calculated in the present
426 study (sediment f_{oc} = 0.5 – 6%),[14] while a field study had found negligible retardation for compounds such
427 as CBZ and BTA during riparian bank filtration (f_{oc} = 0.01-0.11%).[16] Such discrepancies are likely
428 attributable to differences in sediment organic matter content and general sediment heterogeneity.
429 We conclude that reversible sorption processes can substantially retard TrOCs along hyporheic flow paths,
430 even for compounds that are negatively charged. Retardation caused by reversible sorption processes
431 increases the residence time of TrOCs relative to the water residence time in the HZ. Neglecting the effect
432 of retardation may lead to erroneous estimates of removal rate constants, particularly when their
433 calculation is based on simple concentration differences[17] and when sampling periods are relatively short
434 compared to the characteristic time scales over which surface water concentrations fluctuate. Studies that
435 aim at quantitatively investigating the fate of TrOCs in the HZ and along river reaches with significant
436 hyporheic exchange flows should therefore consider retardation and adjust their reactive transport models
437 and sampling schemes accordingly. Some compounds (e.g. CBZ, DBZ, VLX, or DCF) were retarded
438 along the investigated hyporheic flow path but showed only very small removal rates in the HZ. If
439 concentrations of these compounds in surface waters drop considerably over short time scales (e.g. during
440 hydrological events), desorption processes might remobilize TrOCs previously adsorbed to sediment
441 materials and biofilms and hence hyporheic exchange would lead to a concentration increase of these
442 TrOCs in the surface water.
443

3.5 Influence of benthic bio-layer and DOC on TrOC reactivity

For all TrOCs for which concentration changed significantly between the surface water and 40 cm depth in the HZ (22 out of 28) except SMX, removal rates calculated for the top 10 cm in the HZ were substantially higher compared to removal rate constants calculated between 10 and 30 and 30 and 40 cm depth (Figure 3). Because redox conditions in the top 30 cm of the HZ were predominantly oxic, it is reasonable to assume that the increased reactivity in the top 10 cm of the HZ is due to increased microbial activity in the benthic bio-layers growing in the top cm of the HZ and high chemical turnover rates typically associated with shallow hyporheic flow paths.[10,11] This finding is further underlined by changes in DOC concentration and quality, suggesting that TrOC turnover within similar redox zones in the HZ is closely coupled to DOC turnover. Studies on managed aquifer recharge reported that TrOC removal rates under oxic conditions were highest when BDOC was limited, an observation that was mainly attributed to the presence of highly adapted microbial communities that developed under oligotrophic conditions.[22,49,67] However, our results show, that in natural systems such as the HZ, high TrOC removal rates can also be associated with oxic and eutrophic conditions, in which high concentrations of BDOC likely fuel microbial metabolism and serve as a co-substrate for the co-metabolic removal of TrOCs.

Due to practical limitations associated with our sampling approach, the present study investigated a downwelling flow path that is unlikely to return to the surface water. However, our findings should in principle be transferable to hyporheic flow paths that return to the stream and thus have implications for reach-scale removal of TrOCs. Together with earlier investigations showing that for many TrOCs removal rates are higher under oxic compared to anoxic redox conditions,[12,14] our results suggest that short and shallow flow paths are more efficient in removing TrOCs than long and deep flow paths, along which redox conditions become increasingly anoxic and microbial activity decreases. River restoration measures that promote frequent and short vertical exchange flows through the shallow HZ, such as the construction of engineered hyporheic zone elements[68–70] or the application of woody debris,[71] are therefore likely to

468 contribute more to overall in-stream removal of TrOCs than measures that promote, longer lateral
469 exchange flows such as the installation of meander bends or pool-riffle sequences.
470

References

(1) Ternes, T. A.; Joss, A.; Siegrist, H. Peer Reviewed: Scrutinizing Pharmaceuticals and Personal Care Products in Wastewater Treatment. *Environ. Sci. Technol.* **2004**, *38* (20), 392A–399A. https://doi.org/10.1021/es040639t.

(2) Eggen, R. I. L.; Hollender, J.; Joss, A.; Schärer, M.; Stamm, C. Reducing the Discharge of Micropollutants in the Aquatic Environment: The Benefits of Upgrading Wastewater Treatment Plants. *Environ. Sci. Technol.* **2014**, *48* (14), 7683–7689. https://doi.org/10.1021/es500907n.

(3) Bradley, P. M.; Journey, C. A.; Romanok, K. M.; Barber, L. B.; Buxton, H. T.; Foreman, W. T.; Furlong, E. T.; Glassmeyer, S. T.; Hladik, M. L.; Iwanowicz, L. R.; Jones, D. K.; Kolpin, D. W.; Kuivila, K. M.; Loftin, K. A.; Mills, M. A.; Meyer, M. T.; Orlando, J. L.; Reilly, T. J.; Smalling, K. L.; Villeneuve, D. L. Expanded Target-Chemical Analysis Reveals Extensive Mixed-Organic-Contaminant Exposure in U.S. Streams. *Environ. Sci. Technol.* **2017**, *51* (9), 4792–4802. https://doi.org/10.1021/acs.est.7b00012.

(4) Loos, R.; Carvalho, R.; António, D. C.; Comero, S.; Locoro, G.; Tavazzi, S.; Paracchini, B.; Ghiani, M.; Lettieri, T.; Blaha, L.; Jarosova, B.; Voorspoels, S.; Servaes, K.; Haglund, P.; Fick, J.; Lindberg, R. H.; Schwesig, D.; Gawlik, B. M. EU-Wide Monitoring Survey on Emerging Polar Organic Contaminants in Wastewater Treatment Plant Effluents. *Water Res.* **2013**, *47* (17), 6475–6487. https://doi.org/10.1016/j.watres.2013.08.024.

(5) Brodin, T.; Fick, J.; Jonsson, M.; Klaminder, J. Dilute Concentrations of a Psychiatric Drug Alter Behavior of Fish from Natural Populations. *Science* **2013**, *339* (6121), 814–815. https://doi.org/10.1126/science.1226850.

(6) Schwarzenbach, R. P.; Egli, T.; Hofstetter, T. B.; von Gunten, U.; Wehrli, B. Global Water Pollution and Human Health. *Annu. Rev. Environ. Resour.* **2010**, *35* (1), 109–136. https://doi.org/10.1146/annurev-environ-100809-125342.

(7) Arnnok, P.; Singh, R. R.; Burakham, R.; Pérez-Fuentetaja, A.; Aga, D. S. Selective Uptake and

Bioaccumulation of Antidepressants in Fish from Effluent-Impacted Niagara River. *Environ. Sci. Technol.* **2017**, *51* (18), 10652–10662. https://doi.org/10.1021/acs.est.7b02912.

(8) Pal, A.; He, Y.; Jekel, M.; Reinhard, M.; Gin, K. Y. H. Emerging Contaminants of Public Health Significance as Water Quality Indicator Compounds in the Urban Water Cycle. *Environment International*. 2014, *71*, 46–62. https://doi.org/10.1016/j.envint.2014.05.025.

(9) Boano, F.; Harvey, J. W.; Marion, A.; Packman, A. I.; Revelli, R.; Ridolfi, L.; Wörman, A. Hyporheic Flow and Transport Processes: Mechanisms, Models, and Bioghemical Implications. *Rev. Geophys.* **2014**, *52*, 603–379. https://doi.org/10.1002/2012RG000417.Received.

(10) Knapp, J. L. A.; González-Pinzón, R.; Drummond, J. D.; Larsen, L. G.; Cirpka, O. A.; Harvey, J. W. Tracer-Based Characterization of Hyporheic Exchange and Benthic Biolayers in Streams. *Water Resour. Res.* **2017**, *53*, 1575–1594. https://doi.org/10.1002/2016WR019393.

(11) Krause, S.; Lewandowski, J.; Grimm, N. B.; Hannah, D. M.; Pinay, G.; McDonald, K.; Martí, E.; Argerich, A.; Pfister, L.; Klaus, J.; Battin, T.; Larned, S. T.; Schelker, J.; Fleckenstein, J.; Schmidt, C.; Rivett, M. O.; Watts, G.; Sabater, F.; Sorolla, A.; Turk, V. Ecohydrological Interfaces as Hot Spots of Ecosystem Processes. *Water Resour. Res.* **2017**, *53* (8), 6359–6376. https://doi.org/10.1002/2016WR019516.

(12) Burke, V.; Greskowiak, J.; Asmuß, T.; Bremermann, R.; Taute, T.; Massmann, G. Temperature Dependent Redox Zonation and Attenuation of Wastewater-Derived Organic Micropollutants in the Hyporheic Zone. *Sci. Total Environ.* **2014**, *482–483* (1), 53–61. https://doi.org/10.1016/j.scitotenv.2014.02.098.

(13) Li, Z.; Sobek, A.; Radke, M. Flume Experiments to Investigate the Environmental Fate of Pharmaceuticals and Their Transformation Products in Streams. *Environ. Sci. Technol.* **2015**, *49* (10), 6009–6017. https://doi.org/10.1021/acs.est.5b00273.

(14) Schaper, J. L.; Seher, W.; Nützmann, G.; Putschew, A.; Jekel, M.; Lewandowski, J. The Fate of Polar Trace Organic Compounds in the Hyporheic Zone. *Water Res.* **2018**, *140*, 158–166.

https://doi.org/10.1016/j.watres.2018.04.040.

(15) Lewandowski, J.; Putschew, A.; Schwesig, D.; Neumann, C.; Radke, M. Fate of Organic Micropollutants in the Hyporheic Zone of a Eutrophic Lowland Stream: Results of a Preliminary Field Study. *Sci. Total Environ.* **2011**, *409* (10), 1824–1835. https://doi.org/10.1016/j.scitotenv.2011.01.028.

(16) Huntscha, S.; Rodriguez Velosa, D. M.; Schroth, M. H.; Hollender, J. Degradation of Polar Organic Micropollutants during Riverbank Filtration: Complementary Results from Spatiotemporal Sampling and Push-Pull Tests. *Environ. Sci. Technol.* **2013**, *47* (20), 11512–11521. https://doi.org/10.1021/es401802z.

(17) Schaper, J. L.; Posselt, M.; Mccallum, J. L.; Banks, E.; Hoehne, A.; Meinikmann, K.; Shanafield, M.; Batelaan, O.; Lewandowski, J. Hyporheic Exchange Controls Fate of Trace Organic Compounds in an Urban Stream. *Environ. Sci. Technol.* **2018**, *52*, 12285–12294. https://doi.org/10.1021/acs.est.8b03117.

(18) MacKay, A. A.; Vasudevan, D. Polyfunctional Ionogenic Compound Sorption: Challenges and New Approaches to Advance Predictive Models. *Environ. Sci. Technol.* **2012**, *46* (17), 9209–9223. https://doi.org/10.1021/es301036t.

(19) Schaffer, M.; Börnick, H.; Nödler, K.; Licha, T.; Worch, E. Role of Cation Exchange Processes on the Sorption Influenced Transport of Cationic β-Blockers in Aquifer Sediments. *Water Res.* **2012**, *46* (17), 5472–5482. https://doi.org/10.1016/j.watres.2012.07.013.

(20) Writer, J. H.; Antweiler, R. C.; Ferrer, I.; Ryan, J. N.; Thurman, E. M. In-Stream Attenuation of Neuro-Active Pharmaceuticals and Their Metabolites. *Environ. Sci. Technol.* **2013**, *47* (17), 9781–9790. https://doi.org/10.1021/es402158t.

(21) Schaffer, M.; Boxberger, N.; Börnick, H.; Licha, T.; Worch, E. Sorption Influenced Transport of Ionizable Pharmaceuticals onto a Natural Sandy Aquifer Sediment at Different PH. *Chemosphere* **2012**, *87* (5), 513–520. https://doi.org/10.1016/j.chemosphere.2011.12.053.

546 (22) Rauch-Williams, T.; Hoppe-Jones, C.; Drewes, J. E. The Role of Organic Matter in the Removal of
547 Emerging Trace Organic Chemicals during Managed Aquifer Recharge. *Water Res.* **2010**, *44* (2),
548 449–460. https://doi.org/10.1016/j.watres.2009.08.027.
549 (23) Harvey, J. W.; Böhlke, J. K.; Voytek, M. A.; Scott, D.; Tobias, C. R. Hyporheic Zone
550 Denitrification: Controls on Effective Reaction Depth and Contribution to Whole-Stream Mass
551 Balance. *Water Resour. Res.* **2013**, *49* (10), 6298–6316. https://doi.org/10.1002/wrcr.20492.
552 (24) Peralta-Maraver, I.; Galloway, J.; Posselt, M.; Arnon, S.; Reiss, J.; Lewandowski, J.; Robertson, A.
553 L. Environmental Filtering and Community Delineation in the Streambed Ecotone. *Sci. Rep.* **2018**,
554 *8* (October 2017), 1–11. https://doi.org/10.1038/s41598-018-34206-z.
555 (25) Kunkel, U.; Radke, M. Fate of Pharmaceuticals in Rivers: Deriving a Benchmark Dataset at
556 Favorable Attenuation Conditions. *Water Res.* **2012**, *46* (17), 5551–5565.
557 https://doi.org/10.1016/j.watres.2012.07.033.
558 (26) Posselt, M.; Jaeger, A.; Schaper, J. L.; Radke, M.; Benskin, J. P. Determination of Polar Organic
559 Micropollutants in Surface and Pore Water by High-Resolution Sampling-Direct Injection-Ultra
560 High Performance Liquid Chromatography-Tandem Mass Spectrometry. *Environ. Sci. Process.*
561 *Impacts* **2018**, *20* (12), 1716–1727. https://doi.org/10.1039/c8em00390d.
562 (27) Munz, M.; Oswald, S. E.; Schmidt, C. Analysis of Riverbed Temperatures to Determine the
563 Geometry of Subsurface Water Flow around In-Stream Geomorphological Structures. *J. Hydrol.*
564 **2016**, *539*, 74–87. https://doi.org/10.1016/j.jhydrol.2016.05.012.
565 (28) McCallum, A. M.; Andersen, M. S.; Rau, G. C.; Acworth, R. I. A 1-D Analytical Method for
566 Estimating Surface Water-Groundwater Interactions and Effective Thermal Diffusivity Using
567 Temperature Time Series. *Water Resour. Res.* **2012**, *48* (11), 1–8.
568 https://doi.org/10.1029/2012WR012007.
569 (29) Gordon, R. P.; Lautz, L. K.; Briggs, M. A.; McKenzie, J. M. Automated Calculation of Vertical
570 Pore-Water Flux from Field Temperature Time Series Using the VFLUX Method and Computer

571 Program. *J. Hydrol.* **2012**, *420–421*, 142–158. https://doi.org/10.1016/j.jhydrol.2011.11.053.
572 (30) Young, P. C.; Pedregal, D. J.; Tych, W. Dynamic Harmonic Regression. *J. Forecast.* **1999**, *18* (6),
573 369–394. https://doi.org/10.1002/(SICI)1099-131X(199911)18:6<369::AID-FOR748>3.0.CO;2-K.
574 (31) Jaeger, A.; Posselt, M.; Betterle, A.; Schaper, J.; Mechelke, J.; Coll, C.; Lewandowski, J. Spatial
575 and Temporal Variability in Attenuation of Polar Organic Micropollutants in an Urban Lowland
576 Stream. *Environ. Sci. Technol.* **2018**, *53*, 2383–2395. https://doi.org/10.1021/acs.est.8b05488.
577 (32) Zietzschmann, F.; Aschermann, G.; Jekel, M. Comparing and Modeling Organic Micro-Pollutant
578 Adsorption onto Powdered Activated Carbon in Different Drinking Waters and WWTP Effluents.
579 *Water Res.* **2016**, *102*, 190–201. https://doi.org/10.1016/j.watres.2016.06.041.
580 (33) Aschermann, G.; Zietzschmann, F.; Jekel, M. Influence of Dissolved Organic Matter and Activated
581 Carbon Pore Characteristics on Organic Micropollutant Desorption. *Water Res.* **2018**, *133*, 123–
582 131. https://doi.org/10.1016/j.watres.2018.01.015.
583 (34) Ohno, T. Fluorescence Inner-Filtering Correction for Determining the Humification Index of
584 Dissolved Organic Matter. *Environ. Sci. Technol.* **2002**, *36* (4), 742–746.
585 https://doi.org/10.1021/es0155276.
586 (35) Weishaar, J. L.; Aiken, G. R.; Bergamaschi, B. A.; Fram, M. S.; Fujii, R.; Mopper, K. Evaluation
587 of Specific Ultraviolet Absorbance as an Indicator of the Chemical Composition and Reactivity of
588 Dissolved Organic Carbon. *Environ. Sci. Technol.* **2003**, *37* (20), 4702–4708.
589 https://doi.org/10.1021/es030360x.
590 (36) Harvey, R. W.; Garabedian, S. P. Use of Colloid Filtration Theory in Modelling Movement of
591 Bacteria through a Contaminated Sandy Aquifer. *Environ. Sci. Technol.* **1991**, *25*, 178–185.
592 (37) Kunkel, U.; Radke, M. Reactive Tracer Test to Evaluate the Fate of Pharmaceuticals in Rivers.
593 *Environ. Sci. Technol.* **2011**, *45* (15), 6296–6302. https://doi.org/10.1021/es104320n.
594 (38) Vrugt, J. A.; Robinson, B. A.; Clark, M. P.; ter Braak, C. J. F.; Hyman, J. M. Treatment of Input
595 Uncertainty in Hydrologic Modeling: Doing Hydrology Backward with Markov Chain Monte

596 Carlo Simulation. *Water Resour. Res.* **2008**, *44* (12), 1–15. https://doi.org/10.1029/2007wr006720.
597 (39) Vrugt, J. A. Markov Chain Monte Carlo Simulation Using the DREAM Software Package: Theory,
598 Concepts, and MATLAB Implementation. *Environ. Model. Softw.* **2016**, *75*, 273–316.
599 https://doi.org/10.1016/j.envsoft.2015.08.013.
600 (40) Voermans, J. J.; Ghisalberti, M.; Ivey, G. N. A Model for Mass Transport Across the Sediment-
601 Water Interface. *Water Resour. Res.* **2018**, *54* (4), 2799–2812.
602 https://doi.org/10.1002/2017WR022418.
603 (41) Grant, S. B.; Azizian, M.; Cook, P.; Boano, F.; Rippy, M. A. Factoring Stream Turbulence into
604 Global Assessments of Nitrogen Pollution. *Science* **2018**, *359*, 1266–1269.
605 (42) Zarnetske, J. P.; Haggerty, R.; Wondzell, S. M.; Baker, M. A. Dynamics of Nitrate Production and
606 Removal as a Function of Residence Time in the Hyporheic Zone. *J. Geophys. Res. Biogeosciences*
607 **2011**, *116* (1), 1–12. https://doi.org/10.1029/2010JG001356.
608 (43) Mulholland, P. J.; Helton, A. M.; Poole, G. C.; Hall, R. O.; Hamilton, S. K.; Peterson, B. J.; Tank,
609 J. L.; Ashkenas, L. R.; Cooper, L. W.; Dahm, C. N.; Dodds, W. K.; Findlay, S. E. G.; Gregory, S.
610 V.; Grimm, N. B.; Johnson, S. L.; McDowell, W. H.; Meyer, J. L.; Valett, H. M.; Webster, J. R.;
611 Arango, C. P.; Beaulieu, J. J.; Bernot, M. J.; Burgin, A. J.; Crenshaw, C. L.; Johnson, L. T.;
612 Niederlehner, B. R.; O'Brien, J. M.; Potter, J. D.; Sheibley, R. W.; Sobota, D. J.; Thomas, S. M.
613 Stream Denitrification across Biomes and Its Response to Anthropogenic Nitrate Loading. *Nature*
614 **2008**, *452* (7184), 202–205. https://doi.org/10.1038/nature06686.
615 (44) Briggs, M. A.; Day-Lewis, F. D.; Zarnetske, J. P.; Harvey, J. W. A Physical Explanation for the
616 Development of Redox Microzones in Hyporheic Flow. *Geophys. Res. Lett.* **2015**, *42* (11), 4402–
617 4410. https://doi.org/10.1002/2015GL064200.
618 (45) Redeker, M.; Wick, A.; Meermann, B.; Ternes, T. A. Anaerobic Transformation of the Iodinated
619 X-Ray Contrast Medium Iopromide, Its Aerobic Transformation Products, and Transfer to Further
620 Iodinated X-Ray Contrast Media. *Environ. Sci. Technol.* **2018**, *52*, 8309–8320.

https://doi.org/10.1021/acs.est.8b01140.

(46) Schulz, M.; Löffler, D.; Wagner, M.; Ternes, T. A. Transformation of the X-Ray Contrast Medium Iopromide in Soil and Biological Wastewater Treatment. *Environ. Sci. Technol.* **2008**, *42* (19), 7207–7217. https://doi.org/10.1021/es800789r.

(47) Kormos, J. L.; Schulz, M.; Kohler, H. P. E.; Ternes, T. A. Biotransformation of Selected Iodinated X-Ray Contrast Media and Characterization of Microbial Transformation Pathways. *Environ. Sci. Technol.* **2010**, *44* (13), 4998–5007. https://doi.org/10.1021/es1007214.

(48) Henning, N.; Kunkel, U.; Wick, A.; Ternes, T. A. Biotransformation of Gabapentin in Surface Water Matrices under Different Redox Conditions and the Occurrence of One Major TP in the Aquatic Environment. *Water Res.* **2018**, *137*, 290–300. https://doi.org/10.1016/j.watres.2018.01.027.

(49) Hellauer, K.; Karakurt, S.; Sperlich, A.; Burke, V.; Massmann, G.; Hübner, U.; Drewes, J. E. Establishing Sequential Managed Aquifer Recharge Technology (SMART) for Enhanced Removal of Trace Organic Chemicals: Experiences from Field Studies in Berlin, Germany. *J. Hydrol.* **2018**, *563*, 1161–1168. https://doi.org/10.1016/j.jhydrol.2017.09.044.

(50) Trautwein, C.; Kümmerer, K. Incomplete Aerobic Degradation of the Antidiabetic Drug Metformin and Identification of the Bacterial Dead-End Transformation Product Guanylurea. *Chemosphere* **2011**, *85* (5), 765–773. https://doi.org/10.1016/j.chemosphere.2011.06.057.

(51) Trautwein, C.; Berset, J. D.; Wolschke, H.; Kümmerer, K. Occurrence of the Antidiabetic Drug Metformin and Its Ultimate Transformation Product Guanylurea in Several Compartments of the Aquatic Cycle. *Environ. Int.* **2014**, *70*, 203–212. https://doi.org/10.1016/j.envint.2014.05.008.

(52) Bradley, P. M.; Journey, C. A.; Button, D. T.; Carlisle, D. M.; Clark, J. M.; Mahler, B. J.; Nakagaki, N.; Qi, S. L.; Waite, I. R.; VanMetre, P. C. Metformin and Other Pharmaceuticals Widespread in Wadeable Streams of the Southeastern United States. *Environ. Sci. Technol. Lett.* **2016**, *3* (6), 243–249. https://doi.org/10.1021/acs.estlett.6b00170.

(53) Scheurer, M.; Michel, A.; Brauch, H. J.; Ruck, W.; Sacher, F. Occurrence and Fate of the Antidiabetic Drug Metformin and Its Metabolite Guanylurea in the Environment and during Drinking Water Treatment. *Water Res.* **2012**, *46* (15), 4790–4802. https://doi.org/10.1016/j.watres.2012.06.019.

(54) Letzel, T.; Bayer, A.; Schulz, W.; Heermann, A.; Lucke, T.; Greco, G.; Grosse, S.; Schüssler, W.; Sengl, M.; Letzel, M. LC-MS Screening Techniques for Wastewater Analysis and Analytical Data Handling Strategies: Sartans and Their Transformation Products as an Example. *Chemosphere* **2015**, *137*, 198–206. https://doi.org/10.1016/j.chemosphere.2015.06.083.

(55) Nödler, K.; Hillebrand, O.; Idzik, K.; Strathmann, M.; Schiperski, F.; Zirlewagen, J.; Licha, T. Occurrence and Fate of the Angiotensin II Receptor Antagonist Transformation Product Valsartan Acid in the Water Cycle - A Comparative Study with Selected β-Blockers and the Persistent Anthropogenic Wastewater Indicators Carbamazepine and Acesulfame. *Water Res.* **2013**, *47* (17), 6650–6659. https://doi.org/10.1016/j.watres.2013.08.034.

(56) Bertelkamp, C.; Reungoat, J.; Cornelissen, E. R.; Singhal, N.; Reynisson, J.; Cabo, A. J.; van der Hoek, J. P.; Verliefde, A. R. D. Sorption and Biodegradation of Organic Micropollutants during River Bank Filtration: A Laboratory Column Study. *Water Res.* **2014**, *52*, 231–241. https://doi.org/10.1016/j.watres.2013.10.068.

(57) Wiese, B.; Massmann, G.; Jekel, M.; Heberer, T.; Dünnbier, U.; Orlikowski, D.; Grützmacher, G. Removal Kinetics of Organic Compounds and Sum Parameters under Field Conditions for Managed Aquifer Recharge. *Water Res.* **2011**, *45* (16), 4939–4950. https://doi.org/10.1016/j.watres.2011.06.040.

(58) Hellauer, K.; Mergel, D.; Ruhl, A. S.; Filter, J.; Hübner, U.; Jekel, M.; Drewes, J. E. Advancing Sequential Managed Aquifer Recharge Technology (SMART) Using Different Intermediate Oxidation Processes. *Water* **2017**, *9* (221), 1–14. https://doi.org/10.3390/w9030221.

(59) Redeker, M.; Wick, A.; Meermann, B.; Ternes, T. A. Removal of the Iodinated X-Ray Contrast

671 Medium Diatrizoate by Anaerobic Transformation. *Environ. Sci. Technol.* **2014**, *48* (17), 10145–
672 10154. https://doi.org/10.1021/es5014714.
673 (60) Su, T.; Deng, H.; Benskin, J. P.; Radke, M. Biodegradation of Sulfamethoxazole Photo-
674 Transformation Products in a Water/Sediment Test. *Chemosphere* **2016**, *148*, 518–525.
675 https://doi.org/10.1016/j.chemosphere.2016.01.049.
676 (61) Zuehlke, S.; Duennbier, U.; Heberer, T. Investigation of the Behavior and Metabolism of
677 Pharmaceutical Residues during Purification of Contaminated Ground Water Used for Drinking
678 Water Supply. *Chemosphere* **2007**, *69* (11), 1673–1680.
679 https://doi.org/10.1016/j.chemosphere.2007.06.020.
680 (62) Massmann, G.; Dünnbier, U.; Heberer, T.; Taute, T. Behaviour and Redox Sensitivity of
681 Pharmaceutical Residues during Bank Filtration - Investigation of Residues of Phenazone-Type
682 Analgesics. *Chemosphere* **2008**, *71* (8), 1476–1485.
683 https://doi.org/10.1016/j.chemosphere.2007.12.017.
684 (63) Briones, R. M.; Sarmah, A. K. Insight into the Sorption Mechanism of Metformin and Its
685 Transformation Product Guanylurea in Pastoral Soils and Model Sorbents. *Sci. Total Environ.*
686 **2018**, *645*, 1323–1333. https://doi.org/10.1016/j.scitotenv.2018.07.251.
687 (64) Torresi, E.; Polesel, F.; Bester, K.; Christensson, M.; Smets, B. F.; Trapp, S.; Andersen, H. R.;
688 Plósz, B. G. Diffusion and Sorption of Organic Micropollutants in Biofilms with Varying
689 Thicknesses. *Water Res.* **2017**, *123*, 388–400. https://doi.org/10.1016/j.watres.2017.06.027.
690 (65) Ramil, M.; El Aref, T.; Fink, G.; Scheurer, M.; Ternes, T. A. Fate of Beta Blockers in Aquatic-
691 Sediment Systems: Sorption and Biotransformation. *Environ. Sci. Technol.* **2010**, *44* (3), 962–970.
692 https://doi.org/10.1021/es9027452.
693 (66) Tülp, H. C.; Fenner, K.; Schwarzenbach, R. P.; Goss, K. U. PH-Dependent Sorption of Acidic
694 Organic Chemicals to Soil Organic Matter. *Environ. Sci. Technol.* **2009**, *43* (24), 9189–9195.
695 https://doi.org/10.1021/es902272j.

(67) Hoppe-Jones, C.; Dickenson, E. R. V.; Drewes, J. E. The Role of Microbial Adaptation and Biodegradable Dissolved Organic Carbon on the Attenuation of Trace Organic Chemicals during Groundwater Recharge. *Sci. Total Environ.* **2012**, *437*, 137–144. https://doi.org/10.1016/j.scitotenv.2012.08.009.

(68) Herzog, S. P.; Higgins, C. P.; McCray, J. E. Engineered Streambeds for Induced Hyporheic Flow: Enhanced Removal of Nutrients, Pathogens, and Metals from Urban Streams. *J. Environ. Eng.* **2016**, *142* (1), 04015053. https://doi.org/10.1061/(ASCE)EE.1943-7870.0001012.

(69) Herzog, S. P.; Higgins, C. P.; Singha, K.; McCray, J. E. Performance of Engineered Streambeds for Inducing Hyporheic Transient Storage and Attenuation of Resazurin. *Environ. Sci. Technol.* **2018**, *52* (18), 10627–10636. https://doi.org/10.1021/acs.est.8b01145.

(70) Peter, K. T.; Herzog, S.; Tian, Z.; Wu, C.; McCray, J. E.; Lynch, K.; Kolodziej, E. P. Evaluating Emerging Organic Contaminant Removal in an Engineered Hyporheic Zone Using High Resolution Mass Spectrometry. *Water Res.* **2019**, *150*, 140–152. https://doi.org/10.1016/j.watres.2018.11.050.

(71) Blaen, P. J.; Kurz, M. J.; Drummond, J. D.; Knapp, J. L. A.; Mendoza-Lera, C.; Schmadel, N. M.; Klaar, M. J.; Jäger, A.; Folegot, S.; Lee-Cullin, J.; Ward, A. S.; Zarnetske, J. P.; Datry, T.; Milner, A. M.; Lewandowski, J.; Hannah, D. M.; Krause, S. Woody Debris Is Related to Reach-Scale Hotspots of Lowland Stream Ecosystem Respiration under Baseflow Conditions. *Ecohydrology* **2018**, *11* (5), 1–9. https://doi.org/10.1002/eco.1952.

719 **Supporting Information**

720 (1) Additional information on VFLUX 2.0 calculations and (2) TrOC analysis (Tables SI-01 & 02); (3)
721 Description of the reactive transport model, DREAM settings, and molecular diffusion coefficients of
722 TrOCs (Table SI-03); (4) Comparison of table reference compounds (Figure SI-01); (5) Median
723 concentrations of TrOCs, NO_3^--N, dissolved manganese and total dissolved iron in the surface water and
724 in hyporheic porewater; (6) Measured hyporheic temperatures (Figure SI-02) and further discussion on
725 DOC and NO_3^--N dynamics in the HZ (Figures SI-03 & 04); (7) pKa and $LogK_{ow}$ values of investigated
726 TrOCs (Table SI-05); (8) Pearson Product Moment correlations between $logD_{ow}$ and calculated retardation
727 coefficients; (9) Concentration time series and associated model fits (Figures SI-05 - SI-32) of all
728 investigated TrOCs.
729
730
731
732

Acknowledgements

This project has been conducted within the Research Training Group 'Urban Water Interfaces (UWI)' (Project N6 "Retention of chemical compounds in hyporheic reactors of urban freshwater systems", GRK 2032/1), which is funded by the German Research Foundation (DFG). This project has also received funding from the European Union's Horizon 2020 research and innovation programme under grant agreement No. 641939 (HypoTRAIN). We are grateful to three anonymous reviewers and the editor for discussion and comments on earlier versions of this manuscript.

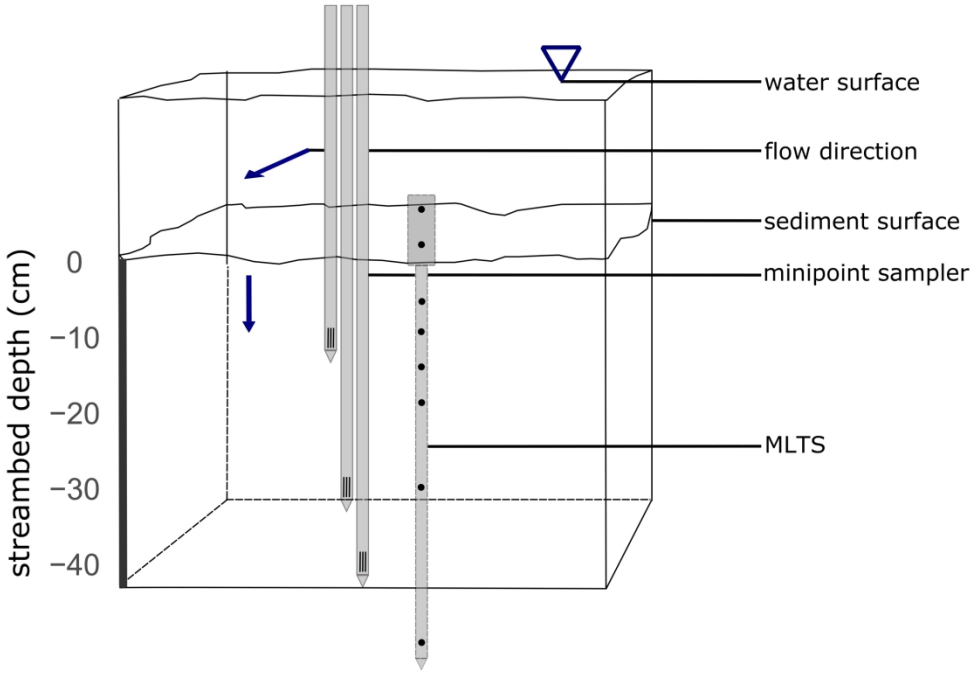
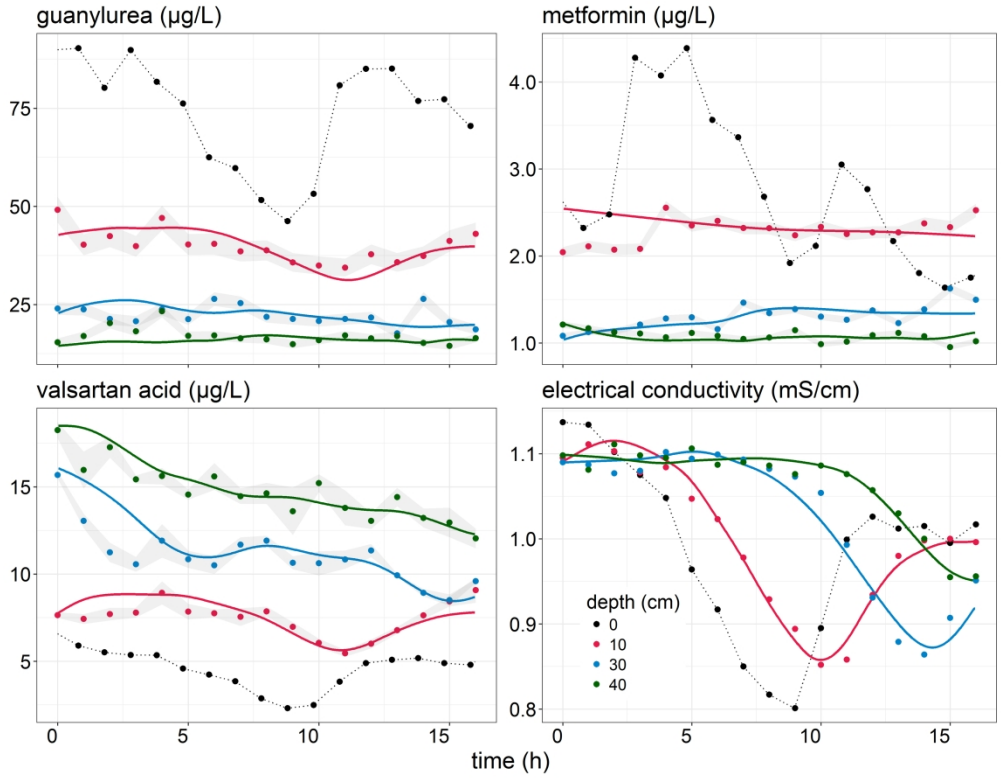


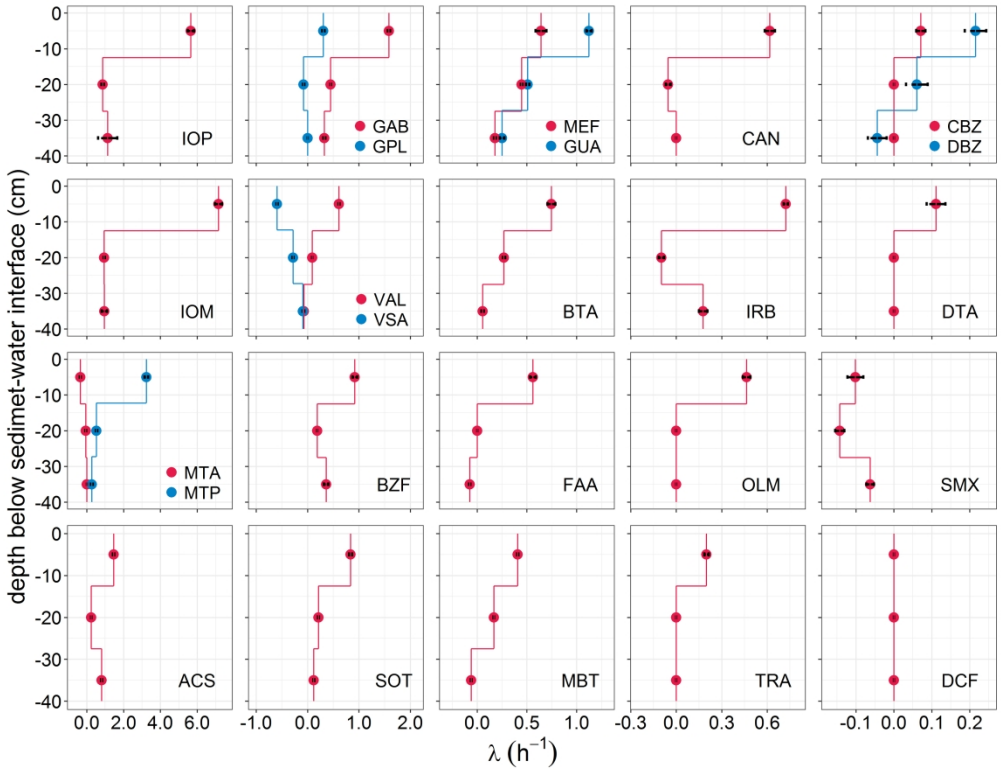
Figure 1 Experimental setup showing the three minipoint sampler installed in 10 cm, 30 cm and 40 cm depth in the hyporheic zone (HZ). The samplers were installed in a line (< 1 cm distance) perpendicular to the water flow direction. A Multilevel Temperature Stick (MLTS) was installed in close proximity (≈ 10 cm) next to the minipoint sampler array. Blue arrows indicate surface water and predominant hyporheic flow directions. Minipoint samplers were sampled from an aluminum bridge spanning the river channel (not shown).

200x139mm (300 x 300 DPI)



Measured (dots) and modeled (solid lines) concentration time series in 10 cm, 30 cm and 40 cm depth in the hyporheic zone (HZ) and measured concentration time series in the surface water (0 cm) of guanylurea (GUA), metformin (MEF), valsartan acid (VSA) and electrical conductivity (EC). For concentration time series measured in the HZ, analytical uncertainty (one standard deviation) is shown in grey. Note that for modeling purposes, concentration time series in the surface water were linearly interpolated (black dashed line) and that for EC no measurement uncertainties were available.

304x243mm (300 x 300 DPI)



First-order removal rate constants (λ) as a function of depth of all investigated parent compounds (PCs, shown in red) and transformation compounds (TPs, shown in blue) except, primidone, epoxy-carbamazepine, venlafaxine and O-desmethylvenlafaxine. Error bars indicate one standard deviation. ACS, acesulfame; BTA, benzotriazole; BZF, bezafibrate; CAN, candesartan; CBZ, carbamazepine; DBZ, dihydroxy-carbamazepine; DCF, diclofenac; DTA, diatrizoic acid; FAA, 4-formylaminoantipyrine; GAB, gabapentin; GPL, gabapentin-lactam; GUA, guanylurea; IOM, iomeprol; IOP, iopromide; IRB, irbesartan; MBT, methylbenzotriazole; MEF, metformin; MTA, metoprolol acid; MTP, metoprolol; olmesartan, OLM; SMX, sulfamethoxazole; SOT, sotalol; TRA, tramadol; VAL, valsartan; VSA, valsartan acid.

304x243mm (300 x 300 DPI)